Publ. Astron. Soc. Japan, **41**, 1095–1106 (1989)

Number Density Evolution of Lyman-Alpha Clouds: Evolving Minihalos

Satoru IKEUCHI and Izumi MURAKAMI

National Astronomical Observatory, Mitaka, Tokyo 181

and

Martin J. REES

Institute of Astronomy, Madingley Road, Cambridge, CB3 0HA, U.K.

(Received 1989 April 26; accepted 1989 August 17)

Abstract

As a model for the Lyman α forest, the evolution of baryon clouds under the potential of cold dark matter, so called minihalos, is examined by taking into account the time variation of diffuse UV flux. After minihalos settle into a stable equilibrium branch they are gradually destabilized due to a decrease in UV flux; finally, they undergo a free-fall collapse, probably leading to the formation of low-mass galaxies. This behavior is related to the observed number density evolution of the Lyman α forest and the mass spectrum of minihalos. A new idea for the inverse effect in relation to this minihalo evolution is also presented.

Key words: Diffuse UV flux; Inverse effect; Lyman α forest; Minihalo model.

1. Introduction

A Lyman α forest yields important information concerning the evolution and structure of the universe at a redshift of $z=4$–2, at a time when quasars and, presumably, galaxies were beginning to form. Such forests are more than one-hundred times more numerous than galaxies, and show no clear correlations in spatial distribution and supercluster-void structures. Lyman α forests may be key objects for understanding cosmological structure.

The observational characteristics of a Lyman α forest are summarized as follows: (i) The H I column density distribution has been approximated as being $dn/dN_{\rm HI}\propto N_{\rm HI}^{-\beta}$, $\beta=1.6$–1.9 (Murdoch et al. 1986, Carswell et al. 1987) for $N_{\rm HI}=10^{13.5}$–$10^{17}\,{\rm cm}^{-2}$. (ii) The number density evolution is well fitted to $dn/dz\propto(1+z)^{\gamma}$, $\gamma\simeq 2.2$ (Hunstead 1988). (iii) The number density decreases rapidly near quasars [called either the inverse effect (Tytler 1987) or the proximity effect (Bajtlik et al. 1988)].

The column density of the Lyman α forests, and their size limit, indicate that the

lines arise from intergalactic clouds with masses of 10^7–$10^8 M_\odot$ and ionized by diffuse UV flux. Since the self-gravity of clouds is too small to confine them, they are usually supposed not to be in gravitational equilibrium; thus, pressure-confined or freely-expanding cloud models have been proposed (Sargent et al. 1980; Ostriker and Ikeuchi 1983; Bond et al. 1988). In both models the clouds are described as expanding and the observed rapid evolution of the number density of the Lyman α forest (Peterson 1978; Murdoch et al. 1986) is attributed to this expansion. Generally speaking, these expanding clouds have difficulty in forming in the usual gravitational instability scenarios for galaxy formation, such as fragmentation theory (Peebles 1980). The explosion hypothesis gives probable sites for cloud formation in expanding shells (Ikeuchi and Ostriker 1986), though the fragments in the shells which result from gravitational instability seem to be too massive for Lyman α clouds.

The other model, in the framework of a cold dark matter (CDM) dominated universe, invokes intergalactic clouds confined by the gravitational potential of CDM "minihalos" (Rees 1986; Ikeuchi 1986). In the CDM scenario, minihalos with a total mass of $10^{7-9} M_\odot$, which failed to form stars because they were stable to gravitational collapse, are natural products, and their spatial distribution is more uniform than that of bright galaxies. In a preceding paper (Ikeuchi et al. 1988; hereafter referred as paper I), we examined the gravitational equilibrium of minihalos under various conditions, and showed that the H I column density distribution can be approximated as $dn/dN_{\rm HI} \propto N_{\rm HI}^{-5/3}$, nearly independent of the cloud mass. As shown in the succeeding paper (Murakami and Ikeuchi 1990) multi-phase minihalos reproduce the H I column density distribution through optically thick systems. Thus, the above-mentioned observational fact (i) is naturally explained.

In the present paper we investigate the evolution of minihalos when the diffuse UV flux varies with time. As is shown in paper I (see also Ikeuchi and Norman 1987), there are two branches for the gravitational equilibria of a minihalo for a given mass, one being stable (the lower density branch) and the other being unstable (the higher density branch). The stable branch is similar to the equilibrium structure of atmosphere of the earth, the pressure gradient within the cloud being balanced by the gravitational force of an external medium (CDM). The unstable branch just corresponds to self-gravitating clouds with an effective adiabatic index $\gamma \leq 1$ (Black 1981). The equilibrium mass of minihalos increases with the central gas density. It reaches a maximum at the critical density and decreases with a further increase in the density. The maximum (or critical) mass depends upon the temperature. Thus, minihalos can evolve if the central density, the total cloud mass and the temperature vary with time. In the following we discuss the evolutionary features of the minihalos by looking at a simple model in which the diffuse UV flux varies, and try to relate our results to the number density evolution of a Lyman α forest. In section 2 we summarize the equilibrium structure by a simple virial argument. In section 3 the minihalo evolution resulting from a decrease in the diffuse UV flux is calculated and compared with the observed number density evolution of a Lyman α forest. In section 4 we discuss the possible "inverse effect" in relation to evolving minihalos.

2. Fundamental Equations and Gravitational Equilibrium of a Minihalo

2.1. *Fundamental Equations*

The dynamical evolution of a spherical minihalo is written as

$$\frac{\partial^2 r}{\partial t^2} = -\frac{1}{\rho_b}\frac{\partial P_b}{\partial r} - \frac{G}{r^2}(M_{b,r} + M_{d,r}) , \tag{1}$$

$$\frac{dM_{i,r}}{dr} = 4\pi r^2 \rho_i , \qquad (i = b, d) , \tag{2}$$

$$P_b = \rho_b kT/m_b , \tag{3}$$

where r is the radial distance from the center, $M_{i,r}$ $(i=b, d)$ is the mass within the radius r of i-th component and b and d denote the quantities of baryons and CDM, respectively. The thermal state of baryons is described as

$$\frac{dP_b}{dt} - \gamma\frac{P_b}{\rho_b}\frac{d\rho_b}{dt} = (\gamma - 1)(H - L) , \tag{4}$$

where γ is the adiabatic index (taken to be $\gamma = 5/3$) and H and L are, respectively, the heating and cooling rate per unit volume. Here, for simplicity we assume the minihalo to be homogeneous and to evolve homologously under the uniformly distributed dark matter. Multiplying equation (1) by $4\pi r^3 \rho_b$ and integrating it from the center ($r=0$) to the surface ($r=R$), the equation of motion for the cloud radius is obtained as

$$\frac{d^2 R}{dt^2} = \frac{5kT}{Rm_b} - \frac{GM_b}{R^2} - \frac{4\pi}{3} GR\rho_d . \tag{5}$$

The temperature is calculated from equation (4) as

$$\frac{d \ln T}{dt} = (\gamma - 1)\left[\frac{d \ln \rho_b}{dt} + \frac{(H - L)m_b}{\rho_b kT}\right] . \tag{6}$$

The evolution of a minihalo with a fixed mass $M_b = 4\pi R^3 \rho_b/3$ is followed by using equations (5) and (6). In calculating H and L, we assume the ionization equilibrium for a gas with a primordial abundance of $n_{\rm H}/n_{\rm He} = 9$ under the diffuse UV flux J to be

$$JG_i n_i = \alpha_{i+1} n_e n_{i+1} , \tag{7}$$

with $(i, i+1) = ({\rm H\,I}, {\rm H\,II})$, $({\rm He\,I}, {\rm He\,II})$ and $({\rm He\,II}, {\rm He\,III})$. The number density of electrons is given by $n_e = n_{\rm HII} + n_{\rm HeII} + 2n_{\rm HeIII}$, and G_i and α_{i+1} are taken from Black (1981). The heating rate by diffuse UV flux can approximately be written as

$$H = \sum_{i = {\rm HI, HeI, HeII}} JG_i \varepsilon_i n_i , \tag{8}$$

where ε_i's are also given by Black (1981). The cooling rate is calculated taking account of collisional ionization, radiative recombination (including dielectric recombination), line emission after collisional excitation, and electron-ion thermal bremsstrahlung as

well as the inverse Compton effect (Black 1981).

2.2. *Gravitational Equilibrium*

Setting $d^2R/dt^2 = dT/dt = d\rho_b/dt = 0$, the gravitational equilibrium of a minihalo is formally given by

$$M_b = \frac{4\pi}{3}\left(\frac{15kT\rho_b^{2/3}}{4\pi G m_b(\rho_b+\rho_d)}\right)^{3/2}, \tag{9}$$

where the temperature is determined by the condition $H=L$. The parameters which characterize each model are the baryon density, ρ_b; CDM density, ρ_d; and diffuse UV flux, J. For later convenience we rewrite them as

$$C \equiv \rho_b/\rho_d\,, \qquad D \equiv \rho_d/\rho_{\rm crit}\,(z=10) \quad \text{and} \quad J = J_0(1+z)^\alpha\,, \tag{10}$$

where $\rho_{\rm crit}$ $(z=10)$ is the closure density at $z=10$. Then, the parameter dependences of mass, radius and H I column density $N_{\rm HI} = Rn_{\rm HI}$ can be written as

$$M_b \propto C(1+C)^{-3/2}D^{-1/2}T^{3/2}\,, \qquad R \propto (1+C)^{-1/2}D^{-1/2}T^{1/2}\,, \quad \text{and}$$
$$N_{\rm HI} \propto C^2(1+C)^{-1/2}D^{3/2}J^{-1}T^{-1/4}\,. \tag{11}$$

In Paper I we assumed the temperature to be constant. Here, since we exactly calculate T under the condition $H=$L, the equilibrium state of a minihalo for a fixed mass changes with different J. In figure 1 we illustrate the loci of constant masses for the gravitational equilibria, equation (9), and of thermal balance $H=L$ for various J by exactly calculating the functions H and L in the ρ_b-T plane. The crossing points of these two lines indicate the dynamical and thermal equilibrium states. Generally, there are two crossing points for a fixed mass and UV flux; the lower density point ($C \ll 1$) is stable and the higher density one ($C \gg 1$) is unstable.

As can be seen, with a decrease in the UV flux the temperature at the stable point decreases, and there is a critical UV flux, $J_{\rm crit}$, below which there are no equilibrium states for a fixed mass. Conversely, when the UV flux increases the stable point moves to a lower density region. That means that the minihalo expands and that the H I column density decreases, so that it escapes detection. Further, with an increase in mass the gravitational equilibrium line goes up and the stable point shifts to a higher density and a lower temperature. As a result, there are no stable equilibrium points if a minihalo mass exceeds a critical value for a fixed UV flux. There are, therefore, two possible causes of the evolution of minihalos: one is a change in the diffuse UV flux, and the other is that of the mass due to merging or gas accretion. In the present paper we examine the former case.

3. Evolution of Minihalos

3.1. *Evolution of Diffuse UV Flux*

Bechtold et al. (1987) examined the time variation of diffuse UV flux by assuming that it is the integrated output from quasars. Their conclusion was that at $z<2.4$ the diffuse UV flux changes as $J=J_0(1+z)^4$ and at $z>2.4$ it stays constant or decreases rapidly with increasing z. These types of behaviour directly reflect the number density

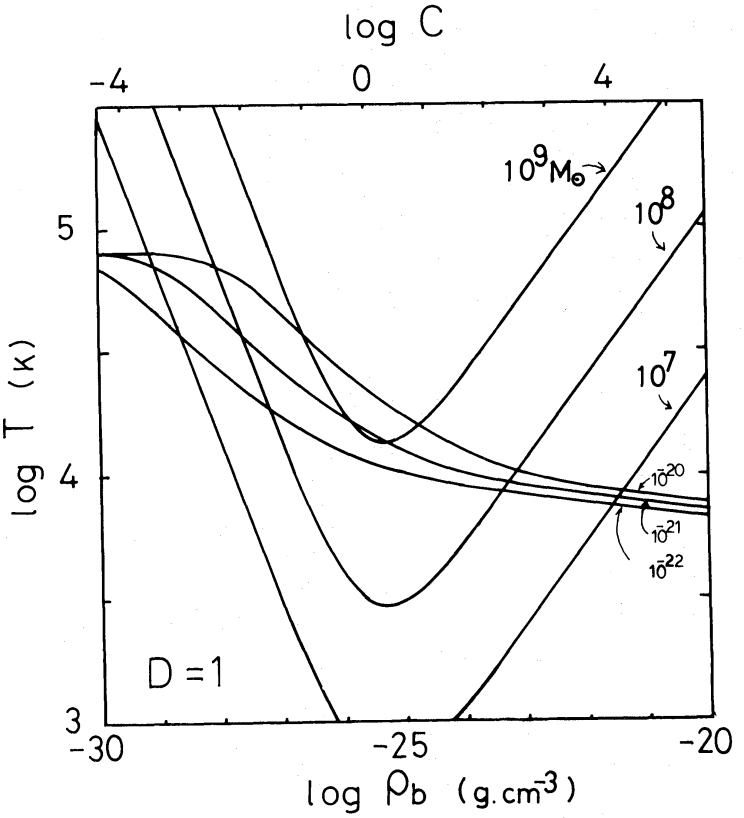

Fig. 1. The loci of constant masses (10^7, 10^8, $10^9 M_\odot$) of minihalos in gravitational equilibrium and of thermal balance $H=L$ for several cases of J (10^{-22}, 10^{-21}, 10^{-20} erg cm^{-2} s^{-1} Hz^{-1}) with $D=1$. The crossing points of two lines indicate the dynamical and thermal equilibrium states.

evolution of quasars. A complication arises because the UV flux is absorbed by H I coulds which are optically thick in the Lyman continuum; moreover, the high-z UV flux may come from sources other than quasars.

Here, we bypass these uncertainties and simply assume the diffuse UV flux changes as

$$J=J_0(1+z)^\alpha\,, \tag{12}$$

where $\alpha=4$ or 2 for all epoch.

As the initial condition at $z=z_i$, we assume a stable equilibrium state with various baryon densities for a fixed D and J_0. In figure 2 we illustrate the equilibrium temperature during the initial epoch. With a decrease in z, the diffuse UV flux decreases. Calculating equations (5) and (6), we can follow the dynamical and thermal evolution of a minihalo.

3.2. *Evolution of Minihalos*

In figure 3 we illustrate the time variations of (a) radii, (b) gas temperatures and (c) H I column densities of minihalos. As expected, a minihalo initially evolves nearly along the equilibrium points; it then collapses after reaching the critical point. The collapsing epoch comes earlier for minihalos with higher C_i for the same D (i.e., more massive), as expected. In figure 4 the epochs of collapse, $1+z_{\rm coll}$, versus the initial gas

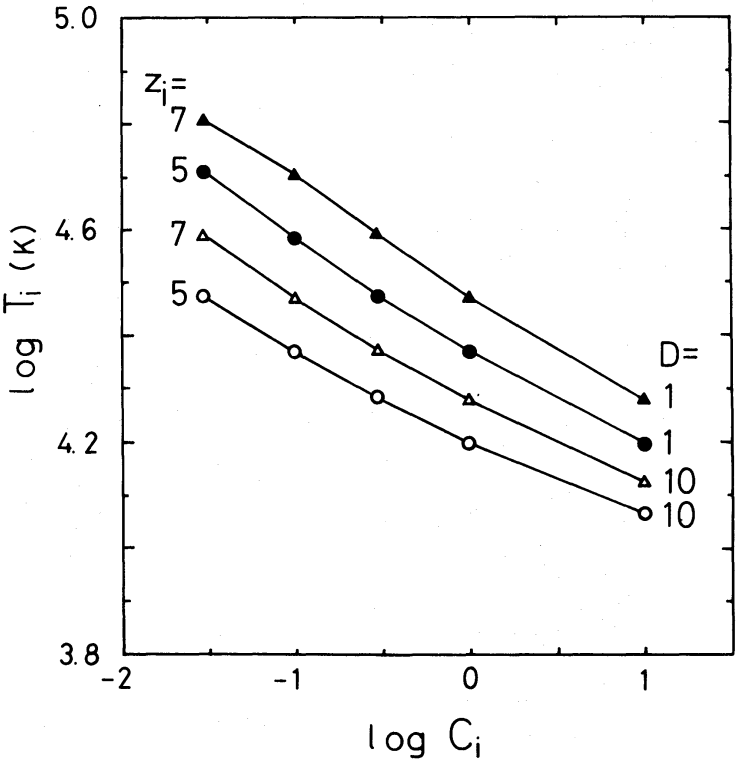

Fig. 2. The equilibrium temperature at the initial epoch, $z_i=7$ (indicated by triangles) or 5 (indicated by circles), for a diffuse UV flux $J_i=10^{-23}(1+z_i)^4$ with respect to the central gas density $C_i=\rho_{b,i}/\rho_d$. For the dark-matter density, ρ_d, we show two cases where D, defined as $\rho_d/\rho_{\rm crit}$ ($z=10$), is 1 and 10, respectively.

density are illustrated for $\alpha=4$ and 2 (by solid and dashed lines, respectively). It is rather interesting that the collapse epoch is simply related to the initial gas density, being closely approximated by $1+z_{\rm coll}\propto\rho_b^{\gamma}(z_i)$, $\gamma=0.12$–0.13 for $\alpha=4$ and $\gamma=0.13$–0.16 for $\alpha=2$. This result can be understood from the following consideration.

For a fixed cloud mass, there is a critical density for a stable minihalo. With a decrease of diffuse UV flux, the temperature decreases and density increases, nearly following the equilibrium line. Soon after, it reaches the critical density and begins to collapse. The evolution of the temperatures is shown in figure 3(b), from which we analytically approximate the z-dependence at $z=2$–4 as

$$T(z)=T_0 M_b^{-x}(1+z)^y\,, \tag{13}$$

where we explicitly describe the mass dependence. Even for the same UV flux, J, the equilibrium temperature depends upon the minihalo mass. In the present model we obtain $x\sim0.25$, independent of α. Then, the density and H I column density can be approximated by

$$\rho_b\propto M_b^{1+3x/2}(1+z)^{-3y/2}\,,\qquad N_{\rm HI}\propto M_b^{2+13x/4}(1+z)^{-\alpha-13y/4}\quad\text{and}$$
$$R\propto T^{1/2}\propto M_b^{-x/2}(1+z)^{y/2}\,, \tag{14}$$

where we assume that the minihalos follow the equilibrium line described by the stable

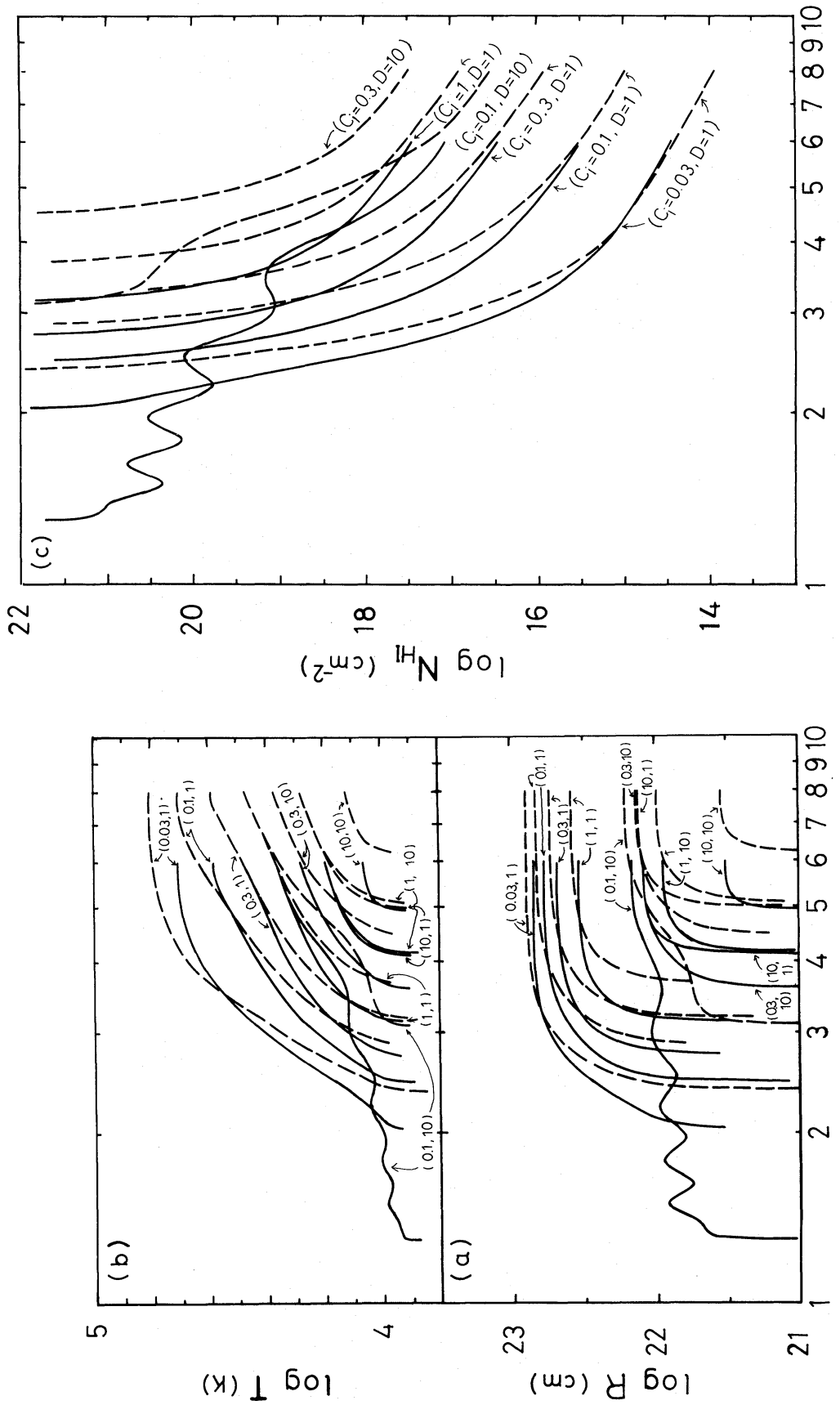

Fig. 3. The evolution of (a) redius R, (b) gas temperature T and (c) H I column density $N_{\rm HI}$ under diffuse UV flux $J=10^{-23}(1+z)^4$ for $z_i=5$ (solid lines) and $z_i=7$ (dashed lines). The set of parameters, (C_f, D), is indicated in each line.

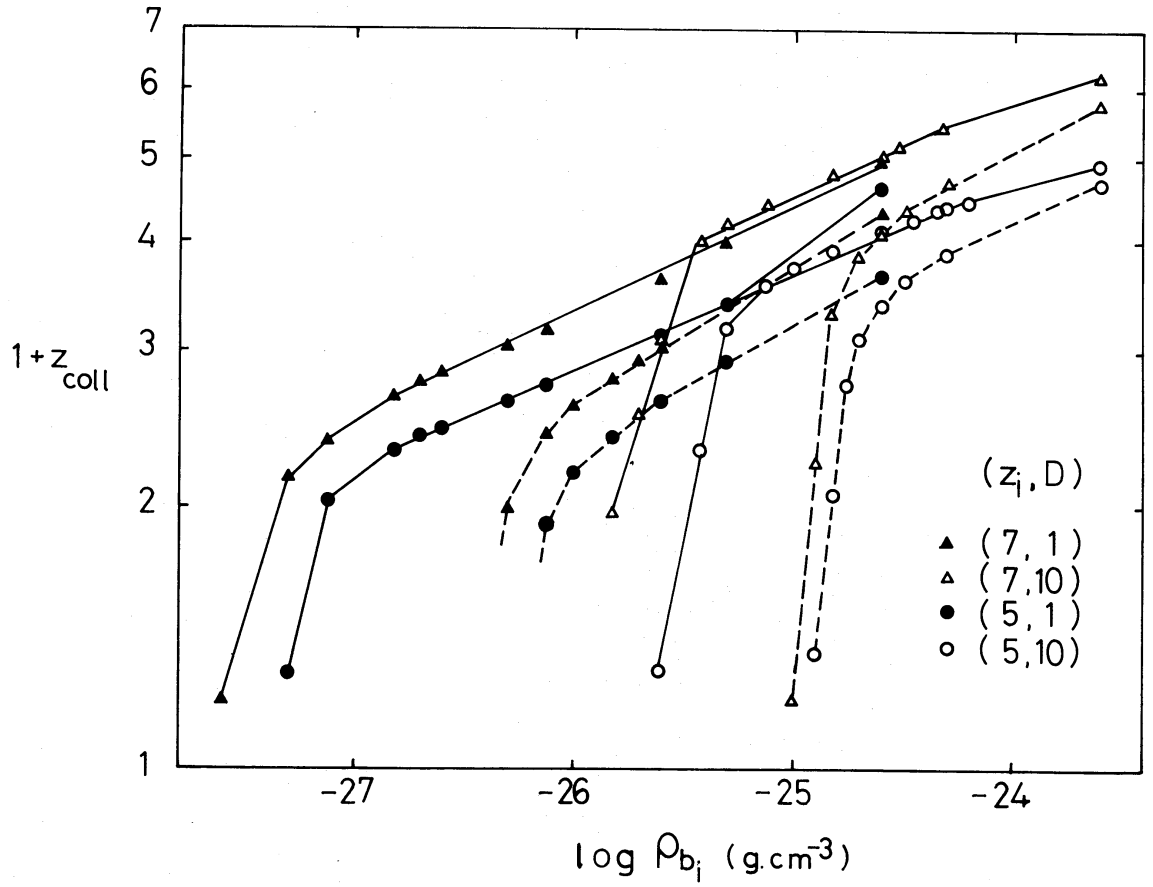

Fig. 4. The collapsing epoch $1+z_{\rm coll}$ of minihalos for the case $J=10^{-23}(1+z)^4$ is indicated by solid lines and for $J=10^{-23}(1+z)^2$ by dashed lines.

branch ($C\ll 1$) in equation (11). For a fixed mass the gas density evolves as

$$\rho_b(z)/\rho_b(z_i)=[(1+z)/(1+z_i)]^{-3y/2}\,. \tag{15}$$

Since the collapse begins when the density reaches the critical value, $\rho_{\rm crit}=\rho_b\sim C_{\rm crit}\cdot\rho_d\sim 2\rho_d$, at which the equilibrium mass (9) becomes maximum, we have

$$(1+z_{\rm coll})=(1+z_i)[\rho_b(z_i)/\rho_{\rm crit}]^{2/3y}\,. \tag{16}$$

The calculated values of y are 5.5 for $\alpha=4$ and 4.4 for $\alpha=2$. The uncertainties of y arise from the deviation of evolutionary tracks from the exact equilibrium states.

As the universe expands, the CDM undergoes hierarchical clustering: small systems form first, and then merge to form higher-mass "halos". The mass spectrum of isolated halos at a given epoch cannot yet be reliably calculated either analytically or numerically. For our present purposes, however, we adopt a simple model in which the mass function of minihalos per unit mass is simply assumed to be a power-law form

$$N_{\rm h}(M_b, z)=\bar{N}(z)M_b^{-\delta}\,. \tag{17}$$

A single power-law can at best be only an adequate approximation over a limited range of mass scales.

The expected number density evolution of observed minihalos can then be written as

$$\frac{dn}{dz}=\left(\frac{dl}{dz}\right)\int_{M_1}^{M_2}\pi R^2 N_{\rm h}(M_b, z)dM_b\,, \tag{18}$$

where l is the mean separation of minihalos, and M_1 and M_2 are the lower and upper mass limits of observable minihalos as a Lyman α forest. Since the H I column density increases with mass, as can be seen in equation (14), the lower mass limit is determined by the detectability of the present technique, $N_{\rm HI}>N_{\rm HI,min}\sim 10^{13.5}\,{\rm cm}^{-2}$. [This constraint is also set in the pressure-confined cloud model by Ikeuchi and Ostriker (1986).] Then, the lower mass limit is given as

$$M_1\propto[N_{\rm HI,min}(1+z)^{\alpha+13y/4}]^{4/(8+13x)}\,. \tag{19}$$

On the other hand, the upper mass limit is given by the condition that the minihalo just begins to collapse at epoch z. From equation (14), this gives rise to

$$M_2\propto[\rho_{\rm crit}(1+z)^{3y/2}]^{2/(2+3x)}\,. \tag{20}$$

Introducing these mass limits and the expression for R into (18) and integrating equation (18), we have

$$\frac{dn}{dz}\sim(1+z)^{1-q_0}(1+z)^{y}(M_2^{-\delta-x+1}-M_1^{-\delta-x+1})/(-\delta-x+1)\,, \tag{21}$$

where we simply write the Hubble constant as $H=H_0(1+z)^{1+q_0}$, which is strictly valid only for $q_0=0$ or $q_0=1/2$. When $\delta>1-x$ and $M_2\gg M_1$, we have

$$\frac{dn}{dz}\propto(1+z)^{\gamma_1}\,,\qquad \gamma_1=1-q_0+y+(4\alpha+13y)(1-x-\delta)/(8+13x)\,. \tag{22}$$

(It can easily be seen that there is no solution for the case $\delta<1-x$.) Then, the power index of the mass spectrum of minihalos become

$$\delta=1-x+(1-q_0+y-\gamma_1)\frac{(8+13x)}{(4\alpha+13y)}\,. \tag{23}$$

The observed number density evolution of the Lyman α forest indicates that $\gamma_1\sim 2.2$, so that we obtain for $q_0=0.5$

$$\delta\sim 1.23\ (\alpha=4)\quad\text{and}\quad 1.22\ (\alpha=2)\,. \tag{24}$$

At present, we can not reliably calculate what mass spectrum is actually predicted in the CDM scenario. It is, however, interesting that the obtained δ is nearly independent of α. This means that the minihalo evolution directly represents the mass spectrum, irrespective of the evolution law of UV flux, so long as α is positive.

If we identify the collapsing minihalos with dwarf galaxies, the number density evolution of dwarf galaxies can be calculated from the upper mass limits as

$$\left(\frac{dn}{dz}\right)_{\rm D}\propto(1+z)^{\gamma_2}\,,\qquad \gamma_2=1-q_0+y+3y(1-x-\delta)/(2+3x)\,. \tag{25}$$

If we use the values in (24) the power index becomes

$$\gamma_2 \sim 2.91 \ (\alpha=4) \quad \text{and} \quad 2.66 \ (\alpha=2) \, . \tag{26}$$

This shows a strong evolution.

The reason for the number density evolution is in complete contrast to what happens in the pressure-confined cloud model. In the minihalo model, the baryon clumps come into contract with decreasing UV flux. The contraction reduces the size of minihalos, though the H I column density increases; thus, less-massive clouds become observable. The former effect decreases the effective cross-sectional area, and the latter increases the number of detectable objects. If the power index of the mass spectrum is around values of (24), the former outweighs the latter and the rapid decrease of detectable clouds can be explained. In the case of pressure-confined clouds, the expansion of clouds increases the detecting area, but a decrease of the H I column density reduces the number of detectable clouds. The latter effect overwhelms the former one.

4. Discussion

4.1. Inverse Effect

As a possible explanation of the inverse effect in a Lyman α forest, Bajtlik et al. (1988) presented the idea that the intensity of UV flux from a quasar exceeds the diffuse UV flux and overionizes the Lyman α clouds. A similar effect is also expected in the present minihalo model. The H I column density at the stable branch is simply expressed as

$$N_{\rm HI} = R \cdot n_{\rm HI} \propto T^{1/2} \cdot \frac{n_b^2 T^{-3/4}}{J} \sim n_b^2 J^{-1} T^{-1/4} \, . \tag{27}$$

It depends upon the UV flux through two effects. One is direct in the sense that a higher UV flux decreases the H I abundance. The other is indirect, in that the higher UV flux increases the temperature and expands the cloud; the fractional H I abundance then decreases due to the slower recombination. Nearer to the quasar the UV flux is intensified and the clouds are so ionized that they are not detectable. In the most extreme case, the lower mass limit exceeds the upper one in equation (18).

In order to clarify this situation, we examine the equilibrium structure of minihalos near a quasar, of which the UV flux, $J_{\rm Q}$, is assumed to exceed the diffuse component. From the numerical result we can approximate the equilibrium temperature as

$$T \sim 3 \times 10^4 M_{b,9}^{-0.3} J_{\rm Q,-21}^{0.2} D^{-0.8} \, {\rm K} \, , \tag{28}$$

where $M_{b,9}$ and $J_{\rm Q,-21}$ are, respectively, the cloud mass in units of $10^9 M_\odot$ and the UV flux from a quasar in units of 10^{-21} erg cm^{-2} s^{-1} Hz^{-1}. The radius and gas density are expressed as

$$R \sim 5.6 \times 10^{22} M_{b,9}^{-0.15} J_{\rm Q,-21}^{0.1} D^{-0.9} \, {\rm cm} \, , \tag{29}$$

and

$$\rho_b \sim 2.7 \times 10^{-27} M_{b,9}^{1.45} J_{\rm Q,-21}^{-0.3} D^{2.7} \, {\rm g \, cm^{-3}} \, . \tag{30}$$

The upper mass limit is obtained by the condition $\rho_b \sim \rho_{\rm crit} \sim 2\rho_d$ as

$$M_2 = 2.8 \times 10^9 J_{\rm Q,-21}^{0.23} D^{-1.31} M_\odot \,. \tag{31}$$

Then, the strong UV flux from a quasar increases the upper mass limit because the gas temperature increases.

On the other hand, the H I column density is given by

$$N_{\rm HI} \sim 5.4 \times 10^{14} M_{b,9}^{3.0} J_{\rm Q,-21}^{-1} J_{\rm Q,-21}^{-0.65} D^{5.1} \,{\rm cm}^{-2} \,, \tag{32}$$

where we show the dependence on $J_{\rm Q}$ dividing into two parts: a direct ionization term and an indirect temperature term. The lower mass limit, corresponding to a cloud with $N_{\rm HI} = 10^{13.5} N_{\rm HI,13.5}\,{\rm cm}^{-2}$, is

$$M_1 \sim 3.9 \times 10^8 N_{\rm HI,13.5}^{0.33} J_{\rm Q,-21}^{0.33} J_{\rm Q,-21}^{0.22} D^{-1.7} M_\odot \,. \tag{33}$$

If $J_{\rm Q}$ increases substantially, this lower mass limit also increases because of high ionization. The expected number density of detectable clouds is expressed as

$$n_{\rm h} \propto \int_{M_2}^{M_2} R^2 M_b^{-\delta} dM_b \propto (M_1^{-\delta+0.7} - M_2^{-\delta+0.7}) J_{\rm Q,-21}^{0.2} D^{-1.8} \,. \tag{34}$$

Adopting $\delta \sim 1.2$ and $N_{\rm HI,13.5} = 1$, this reduces to

$$n_{\rm h} \propto (1 - 0.37 J_{\rm Q,-21}^{0.17} D^{-0.2}) J_{\rm Q,-21}^{-0.08} D^{-0.95} \,. \tag{35}$$

It is interesting that the detectable cloud number is insensitive to $J_{\rm Q}$. Since $M_1^{-\delta}$ decreases, but R^2 increases, with increasing $J_{\rm Q}$, these effects are mutually cancelled out. Then, if $J_{\rm Q,-21} > 500 D^{1.25}$, the value within the parentheses in (35) becomes negative and no clouds are detectable. The UV flux from a quasar is formally written as

$$J_{\rm Q,-21} \simeq 0.9 L_{\nu,31} d_{10}^{-2} \,, \tag{36}$$

where $L_{\nu,31}$ is the intrinsic Lyman-limit luminosity in units of $10^{31}\,{\rm erg\,s^{-1}\,Hz^{-1}}$ and d_{10} is the distance from the quasar in units of 10 Mpc. Therefore, the Lyman clouds are not detectable within $d = 8$ Mpc if $L_\nu > 4 \times 10^{33}\,{\rm erg\,s^{-1}\,Hz^{-1}}$ and $D = 1$, a situation which is highly probable. In a succeeding paper we plan to compare this proximity effect by using more realistic models of minihalos.

4.2. *Implication*

The power index for the mass spectrum obtained in equation (24) indicates that the mass function of dwarf galaxies would be $\bar{N}(M_b) \sim M_2^{-\delta}$ with $\delta \sim 1.2$. If the luminosity is proportional to the mass, the resultant luminosity function corresponds to the faint end of the Schechter function. At least, this fact supports the view that the Lyman α clouds were formed in association with faint galaxies. Then, the Lyman α systems with high column densities may show some spatial correlation.

In the present paper we assume that the UV flux changes as $J = J_0(1+z)^\alpha$ for any epoch. At redshift $z > 2.4$, the actual behavior of J is less certain. Moreover, at all epochs we would expect additional evolutionary effects due to the accretion and dissipative cooling of baryons. Also, self-shielding may be important near the centers; this is important for interpreting the high column density ($> 10^{17}\,{\rm cm}^{-2}$) absorption

lines. Further studies of these effects should clarify the transition between clouds and faint galaxies.

The authors would like to thank H. Suzuki for her careful wordprocessing. Numerical calculations are done in the Data Processing Center of National Astronomical Observatory of Japan.

References

Bajtlik, S., Duncan, R. C., and Ostriker, J. P. 1988, *Astrophys. J.*, **327**, 570.
Bechtold, J., Weymann, R. J., Lin, Z., and Malkan, M. A. 1987, *Astrophys. J.*, **315**, 180.
Black, J. H. 1981, *Monthly Notices Roy. Astron. Soc.*, **197**, 553.
Bond, J. R., Szalay, A. S., and Silk, J. 1988, *Astrophys. J.*, **324**, 627.
Carswell, R. F., Webb, J. K., Baldwin, J. A., and Atwood, B. 1987, *Astrophys. J.*, **319**, 709
Hunstead, R. W. 1988, in *QSO Absorption Lines*, ed. J. C. Blades, D. Turnshek and C. A. Norman (Cambridge University Press, Cambridge), p. 71.
Ikeuchi, S. 1986, *Astrophys. Space Sci.*, **118**, 509.
Ikeuchi, S., Murakami, I., and Rees, M. J. 1988, *Monthly Notices Roy. Astron. Soc.*, **236**, 21 (paper I).
Ikeuchi, S., and Norman, C. A., 1987, *Astrophys. J.*, **312**, 485.
Ikeuchi, S., and Ostriker, J. P. 1986, *Astrophys. J.*, **301**, 522.
Murakami, I., and Ikeuchi, S. 1990, submitted to Publ. Astron. Soc. Japan Letters.
Murdoch, H. S., Hunstead, R. W., Pettini, M., and Blades, J. C. 1986, *Astrophys. J.*, **309**, 19.
Ostriker, J. P., and Ikeuchi, S. 1983, *Astrophys. J. Letters*, **268**, L63.
Peebles, P. J. E. 1980, *The Large Scale Structure of the Universe* (Princeton University Press, Princeton), chapter II.
Peterson, B. A. 1978, in *The Large Scale Structure of the Universe*, *IAU Symp. No. 79*, ed. M. S. Longair and J. Einasto (D. Reidel Publishing Company, Dordrecht), p. 389.
Rees, M. J. 1986, *Monthly Notices Roy. Astron. Soc.*, **218**, 25p.
Sargent, W. L. W., Young, P. J., Boksenberg, A., and Tytler, D. 1980, *Astrophys. J. Suppl.*, **42**, 41.
Tytler, D. 1987, *Astrophys. J.*, **321**, 69.